Magnetic properties of Fe[65](Ni[1-x]Mn[x])[35] ternary alloys(Dissertation_全文)

AUTHOR(S):

Shiga, Masayuki

CITATION:

Shiga, Masayuki. Magnetic properties of Fe[65](Ni[1-x]Mn[x])[35] ternary alloys. 京都大学, 1967, 理学博士

ISSUE DATE:

1967-03-23

URL:

https://doi.org/10.14989/doctor.r905

27

学位申請論文

志賀正幸

主　論　文

Magnetic Properties of $Fe_{65}(Ni_{1-x}Mn_x)_{35}$ Ternary Alloys

Masayuki SHIGA

Department of Metal Science and Technology

Kyoto University, Kyoto, Japan

(Received Sep. 2, 1966)

Magnetic properties of $Fe_{65}(Ni_{1-x}Mn_x)_{35}$ ternary alloys which have the f.c.c. structure over the whole range of x were investigated. It was found that the alloys are antiferromagnetic in the composition range of $1 \geq x > 0.3$ and are ferromagnetic in the composition range of $0 \leq x < 0.3$. In the ferromagnetic region, the Curie temperature and the spontanious magnetization decrease rapidly with increasing x or with the decrease of mean electron concentration. Many physical properties of the alloys are discussed on the basis of three

postulates, i.e., 1) electrons at Mn sites have itinerant character, 2) electrons at Ni sites have localized character and 3) at Fe sites, electrons have itinerant character in the antiferromagnetic range and localized character in the ferromagnetic range. The relation between the atomic distance and the magnetic moment is discussed. The origin of the Invar effect is qualitatively explained on these bases.

§ 1. Introduction

As results of recent investigations[1,2], it became evident that a f.c.c. iron is antiferromagnetic. It is known, however, that γ-iron alloys with other 3d metals have different magnetic properties depending upon the element of solute. Face centered cubic FeMn alloys, for example, are antiferromagnetic[3~6]. On the other hand, nickel rich FeNi alloys are typically ferromagnetic. However, iron rich f.c.c. FeNi alloys which are called as the "Invar alloy" have many anomalous magnetic properties[8~10].

Kondorsky and Sedov[3] explained the Invar anomalies on the basis of an assumption that the exchange integral of electrons of neighbouring ions of iron in a f.c.c. lattice is negative which entails a "latent antiferromagnetism" in the Invar alloy. In order to explain the anomalies of the Invar alloy, on the other hand, Weiss[9] assumed the existence of two electronic states in γ-iron, one of which (γ_1 state) is antiferromagnetic and realized, for example, in FeMn alloys and another one (γ_2 state) is ferromagnetic and realized, for example, in nickel rich FeNi alloys. The stability of the states depends upon a sort and amount of the solute. In the case of the Invar alloy, the γ_2 state might be a ground state and the γ_1 state could be thermally excited. He showed that many anomalies of the Invar alloy could be quantitatively explained by the thermal excitation of the γ_1 state.

Thus , the electronic structure or the type of magnetic coupling

of iron atoms in f.c.c. alloys is determined not only by the sort of the element of solute but also must be dominated by its concentration. Thinking both factors collectively, we take a mean electron concentration or electron/atom ratio as a factor determining the electronic structure or the type of magnetic coupling. Unfortunately, we can not find any f.c.c. iron binary alloy system having electron/atom ratio near 8, where a drastic change of magnetic properties is expected. However, we need not limit the number of solute elements to two, since we took the mean electron concentration as the factor. Then, a ternary iron alloy system will be worthwhile to study the problems. Among them, the investigation of magnetic properties of the alloys $Fe_Y(Ni_{1-X}Mn_X)_{1-Y}$ would bring valuable information about the electronic structure of γ-iron and also the origin of the Invar effect, if this alloy system realizes stable f.c.c. alloys covering a wide range of electron concentration, containing 8 electron/atom region. Nickel and manganese are chosen for the reasons as follows: 1) The valence difference from iron is small. 2) Magnetic properties of f.c.c. FeNi and FeMn alloys have been well investigated. The iron composition Y of these alloys was adjusted as 65 atomic percent to satisfy two contradictive factors as follows: 1) Since one of main purposes of the present investigation is to obtain information about γ-iron itself, it is desired to get f.c.c. alloys containing iron as rich as possible. 2) The alloy containing too much iron does not exist in the form of f.c.c. structure because of metallurgical limitation. In this

paper, the results of X-ray studies and magnetic measurement of $Fe_{65}(Ni_{1-x}Mn_x)_{35}$ alloys are given and the electronic structure of these alloys and the origin of Invar effect are discussed.

§ 2. Experimental Procedures

All of the alloys were prepared by melting together pure electrolytic iron and ingots of NiMn alloys having desired composition in an industion furnace using alumina crucibles and an atmosphere of argon. Bulk samples for magnetic measurements were cut from the ingots. Since some of nickel rich alloys are ferromagnetic, small spherical samples were prepared for measurements of magnetization at 4.2°K so that a demagnetizing field can be correctly estimated. All of the samples were sealed in evacuated quartz tubes and given a homogenizing anneal at 1000°C for two days. Composition were determined by chemical analysis, results of which are given in Table I. The iron composition of all alloys settles between 65 and 66 atomic percent. Therefore, the composition of alloys is correctly expressed by the formula $Fe_{65}(Ni_{1-x}Mn_x)_{35}$. X-ray diffraction studies of the fillings, which were given the same heat treatment, revealed that there is not any phase other than f.c.c. and, at the same time, the lattice constant was determined. Magnetic measurements were made by means of a torsion magnetometer above liquid nitrogen temperature up to about 1000°K. Measurements below liquid nitrogen temperature down to 1.3°K were made by using Bozorth type magnetometer[11]. Magnetization measurement were

made at around the Curie temperature and the exact Curie temperature was determined by means of the $\sigma^2 - H/\sigma$ plotting.

§ 3. Experimental Results

3.1. Lattice constant

The lattice constant of the alloys are given in Fig. 1. It must be noted that the lattice constant decreases linearly with the decrease of manganese concentration in the range of $0.2 \leq x \leq 1.0$ and increases abruptly in the range of $x < 0.2$. Two arrows in Fig.1 indicate the composition where a magnetic transition occurs at room temperature. The position of the left arrow coincides with the composition having almost minimum value of the lattice constant. Since the alloys on the left side of this point are ferromagnetic at room temperature, the extra increase of the lattice constant in this region is attributable to the occurrence of ferromagnetism. This change of the lattice constant caused by the occurrence of ferromagnetism can be estimated from the difference between the observed value and the extrapolated value from the linear part of the graph. A relative value of this expansion thus obtained is 4.2×10^{-3} in length at $20^{\circ}C$ for the alloy of $x=0$. This value can be estimated from another method, i.e., from the analysis of thermal expansion measurement. As is well known, the thermal expansion coefficient of the Invar alloy is very small from around room temperature up to the Curie temperature. Above the Curie temperature, it has ordinary value and a length versus temperature curve is

almost linear. When this linear part of thermal expansion is extrapolated to room temperature, we may regard the difference between this value and the observed one as magnetic expansion. The relative value of this difference at 20°C was estimated as 4.0×10^{-3} in length, where thermal expansion data by Lohr and Hopkins[12] were used. Both values are in good agreement.

On the other hand, any anomaly was not recognized within experimental error near the right arrow, which indicates the boundary of antiferromagnetic (right hand side) and paramagnetic (left hand side) regions. This means that the occurrence of antiferromagnetic ordering does not accompany so large volume change as the Invar alloy. This fact is consistent with the experimental result of temperature dependence of the lattice constant of the FeMn alloy[6], since the expected value of volume change caused by the magnetic ordering is smaller than that of the Invar alloy by order of one.

3.2. Magnetic properties

a) $0 \leq x \leq 0.23$

The experimental results of the temperature dependence of magnetization and inverse susceptibility were given in Fig. 2. In this composition range, alloys are apparently ferromagnetic. The Curie temperature and the saturation magnetization decrease with increasing x. In order to obtain an exact value of the spontanious magnetization at H=0, Measurements of field dependence of magnetization were carried out at liquid helium temperature.

The results are given in Fig. 3. The average magneton number per atom extrapolated to H=0 at 4.2°K was obtained from this results (Fig. 4). The susceptibility above the Curie temperature obeys the Curie-Weiss law for the alloys of $x \leq 0.12$. Figure 4 shows the effective Bohr magneton number obtained from the Curie-Weiss constant and the average magneton number obtained from the spontanious magnetization at 4.2°K. In this figure, the mean electron concentration of the alloys N is taken as abscissa as well as x. The magneton number of FeNi alloys obtained by Crangle and Hallam[13] is given as a function of mean electron concentration. It is rather surprising that the both results lie on a common line. Figure 5 shows the Curie temperature versus x and also the Néel temperature versus x.

b) $x \geq 0.35$

Neutron diffraction studies[6,7] confirmed that f.c.c. FeMn alloys, which corresponds to x=1.0 in the present ternary alloy, are antiferromagnetic. Antiferromagnetism of this alloy shows peculiar characteristics[4,6], for example, the susceptibility above the Néel temperature is nearly temperature independent. This fact suggests itinerant character of 3d electron in this alloy. When manganese is substituted by nickel, on the other hand, the susceptibility increases and becomes temperature dependent as shown in Figs. 6 and 7. This may be interpreted in terms of localization of spins at nickel sites. However, a quantitative treatment is difficult because of ambiguity of estimation of the constant.

paramagnetic susceptibility of matrix alloy. It should be noted that the temperature dependence of the susceptibility is quite similar to that of a usual ionic antiferromagnet and a sharp peak is observed at the Néel temperature. The inverse susceptibility versus temperature curves obey the Curie-Weiss law above $400^{\circ}K$ for the alloys of $x \leq 0.5$. The Néel temperature is given in Fig. 5 as a function of x and N. The Néel temperature of FeMn alloys is also given in Fig. 5 as a function of N.

c) $x \simeq 0.3$

When the curves of composition dependence of the Curie and Néel temperature, which are given in Fig. 5, are extrapolated to lower temperature region, they will cross each other near $x=0.3$. Therefore, it is interesting how the alloys behaves magnetically in this composition range. A sample result of magnetic measurements is given in Fig. 8. The temperature dependence of magnetization has ferromagnetic character above $20^{\circ}K$, but the magnetization falls abruptly when a temperature becomes lower than 20 K. This fall of the magnetization can be interpreted in terms of existence of antiferromagnetic ordering. Then, we can expect the coexistence of antiferromagnetism and ferromagnetism in this alloy. In fact, an exchange anisotropy was found in this alloy at a low temperature. Details will be mentioned in another paper[14].

§ 4. Discussion

As the results of magnetic measurements, it became evident that the magnetic properties of $Fe_{65}(Ni_{1-x}Mn_x)_{35}$ ternary alloy system change markedly with x. The main features which emerged are as follows: 1) The type of magnetic ordering changes from ferromagnetic ($o \lesssim x < 0.3$) to antiferromagnetic ($0.3 < x \lesssim 1$). The Curie Temperature and the spontanious magnetization decrease monotonically with increasing x. The Néel temperature decreases almost linearly with decreasing x. 2), a) The susceptibility above the Curie or the Néel temperature is temperature independent for x=0. b) With decreasing x, it becomes temperature dependent, c) In the ferromagnetic alloys, it obeys the Curie-Weiss law. It seems difficult to explain these facts withing the limit of the localized model. Especially, 2),a) suggests itinerant character of 3d electron in FeMn alloys.

On the other hand, Bailyn[15] gave a theoretical attempt to classify magnetic moment in 3d transition metals and alloys into two types, i.e., an induced moment, which is essentially band type magnetization, and a permanent moment, which is essentially the same as Anderson's localized moment. The permanent moment generally accompanies more or less the induced moment. The intra-atomic correlation energy is the main factor to decide whether the local moment is the permanent or the induced. Of course the stronger is the correlation energy, the more easily the permanent moment state occurs. Now,we shall see that many characteristics

of the present alloy system can be understood by introducing three postulates as follows:.

1) The local moment at manganese sites is always "induced moment".

2) The local moment at nickel sites is always "permanent moment"

3)-a) The local moment at iron sites is "induced moment" in antiferromagnetic alloys and is "permanent moment" in ferromagnetic alloys.

3)-b) At iron sites in the Invar alloy, a substantial amount of local moment is induced below the Curie temperature in addition to the permanent moment.

Recently, Beeby[16] showed that a correlation energy in transition metals increases with electron/atom ratio. His result supports the present postulates 1) and 2) because electron/atom ratio and also the correlation energy increase in the order of Mn < Fe < Ni and it is generally accepted that a large correlation energy causes a localized moment state or the permanent moment state. The postulate 3)-a) is somewhat optional. An internal field at iron nuclei was determined as about 50 kOe for the antiferromagnetic alloy of x= 0.4 at liquid helium temperature by a preliminary Mössbauer experiment[17]. Assuming this small internal field is characteristic to the induced moment, this fact is consistent with the postulate 3)-a). The postulate 3)-b) is strongly supported by paramagnetic scattering of neutron by the Invar alloy[18]. According to Bailyn, a substantial amount of local moment is induced in addition to the permanent moment near the critical condition which distinguishes the

permanent moment state from the induced moment state. We may consider the iron atom in the Invar alloy to be in this condition, since the Invar alloy has the composition near the boundary between the ferromagnetic and antiferromagnetic range or near the critical for the permanent moment state. Then, the increase of the local moment is expected below the Curie temperature. Thus, we may regard the postulates 3)-a) and -b) as dependent one another.

Now, many experimental results can be interpreted in terms of this model as follows.

4.1. Susceptibility above the magnetic ordering temperature

The magnetic susceptibility of f.c.c. FeMn alloys is almost temperature independent above the Néel temperature. This fact is hardly understood from the locatized spin model and suggests an absence of localized moment in the paramagnetic phase as assumed by the postulates. On the other hand, the susceptibility of FeNi alloys obeys the Curie-Weiss law above the Curie temperature. It is consistent with the postulates 2) and 3)-a). In the case of FeNiMn alloys, an addition of nickel makes the susceptibility temperature dependent above the Néel temperature. This can be understood from the spin localization at nickel sites. It must be noted that the susceptibility of FeNiMn alloys, for example x=0.4, have a very sharp peak at the Néel temperature. This probably means that antiferromagnetic coupling force spreads over long range distance and a spin ordering temperature is little affected by local fluctuation of composition. The long range force

is naturally expected from itinerant character of 3d electron.

4.2. Paramagnetic scattering of neutron and electron by spins

Recently, Collins[18] made a study of paramagnetic scattering of neutron by the Invar alloy. Fairly large scattering was observed at far above the Curie temperature. The mean value of the atomic moment was estimated as $1.4\mu_B$ and it is temperature independent. This result indicates the existence of localized moment in the paramagnetic phase, at least for longer period of time than passing time of neutron. The mean magnetic moment in the ferromagnetic phase is estimated as about $2.2\mu_B$[18], which is larger than that in the paramagnetic phase by $0.8\mu_B$. We may consider this extra moment as induced one by ferromagnetic molecular field as expected from postulate 3)-b). Paramagnetic scattering of neutron by FeMn alloy is comparatively small[19] ($\simeq 0.5\mu_B$). We may regard the large difference of paramagnetic scattering between both alloys as an evidence of the validity of our model.

A similar effect was observed in the magnetic disorder resistance caused by scattering of electron by spins. The mean value of magnetic moment in the paramagnetic phase can be roughly estimated by means of the analysis developed by Weiss and Marotta[20]. We got the value of about $1.8\mu_B$ for the 35 percent nickel FeNi alloy and $0.4\mu_B$ for the 35 percent manganese FeMn alloy, where the data of resistivity measurement by Shiga and Nakamura [4] for FeMn and by Shirakawa[21] for FeNi alloy were used. The results of neutron and resistivity studies are in good agreement.

4.3. The origin of the Invar effect and an atomic distance

Weiss[9] gave an elabolate explanation on the origin of the Invar effect assuming the existence of two electronic state (γ_1, γ_2) in the γ-iron. The present model is somewhat analogous to Weiss': The induced moment state corresponds to the γ_1 state and the permanent moment state to the γ_2 state. However, the temperature dependence of the magnetic moment obtained by neutron scattering is somewhat different from what is predicted by Weiss' model. Lattice constant of FeNiMn alloys, on the other hand, changes abruptly near x=0.2, where the Curie temperature is just at room temperature. Moreover, the coefficient of thermal expansion of the Invar alloy changes discontinuously just below the Curie temperature[22]. These facts indicate the ferromagnetic origin of the extra increase of lattice constant in contrast to Weiss' model. In the section 4.2., we discussed the increase of local moment of iron atoms in the Invar alloy below the Curie temperature. If we assume that the increase of the magnetic moment accompanies an increase of atomic distance, so called Invar effect is qualitatively explained by the present postulates. Now, let us discuss the above mentioned assumption on the relation between the magnetic moment and the atomic distance. In the condition of the perfectly magnetized state of local moment, the Wannier function with up - spin at the corresponding atomic sites is fully occupied, so that the upper part of 3d band with antibonding character must be occupied. On the contrary, in the delocalized state or the weakly polarized

state, the occupation of the electronic state with antibonding character can be avoided, especially when orbitals are nearly half filled. The more strongly the occupied state has antibonding character, the larger atomic distance is expected. Thus, we got a resonable explanation for the assumption on the relation between the magnetic moment and the atomic distance, i.e., the larger the atomic moment, the larger the atomic distance. On the other hand, the most important characteristic of the Invar effects is the large volume change caused by ferromagnetic ordering. This effect is understood from the above arguments.

Acknowledgments

The auther wish to express his thanks to Professor Y. Nakamura for encouragements and instructive discussions and Professor H. Takaki and members of his laboratory for usefull discussions. Thanks are due to IBM Thomas J. Watson Research Center for measurement of magnetization at low temperature and also to Dr. J. Matsuoka for chemical analysis of the alloys.

References

1) S. C. Abrahams, L. Guttman and J. S. Kasper: Phys. Rev. 127 (1962) 2052.

2) U. Gonser, C. J. Meechan, A.H. Muir and H. Wiedersich: J Appl. Phys. 34 (1963) 2373.

3) V. L. Sedov: Sov. Phys. JETP 15 (1962) 88.

4) M. Shiga and Y. Nakamura: J. Phys. Soc. Japan 19 (1964) 1743.

5) C. Kimball, W. D. Gerber and A. Arrott: J. Appl. Phys. 34 (1963) 1046.

6) H. Umebayashi and Y. Ishikawa: J. Phys. Soc. Japan 21 (1966) 1281.

7) J. S. Kouvel and J.S. Kasper: J. Phys. Chem. Solids 24 (1964) 1743.

8) E. I. Kondorsky and V.L. Sedov: J. Appl. Phys. 31 (1960) 331s.

9) R. J. Weiss: Proc. Phys. Soc. 82 (1963) 2811.

10) Y. Nakamura, M. Shiga and N. Shikazono: J. Phys. Soc. Japan 19 (1964) 1177.

11) R. M. Bozorth, H. J. Williams and D. E. Walsh: Phys. Rev. 103 (1956) 572.

12) J. M. Lohr and C. H. Hopkins: Trans. AIMME 135 (1939) 535.

13) J. Crangle and G. C. Hallam: Proc. Roy. Soc. A272 (1963) 119.

14) Y. Nakamura and N. Miyata: to be Published.

15) M. Bailyn: Phys. Rev. 139 (1965) A1905.

16) J. L. Beeby: Phys. Rev. 141 (1966) 781.

17) M. Shiga et al: to be published.

18) M. F. Collins: Proc. Phys. Soc. 86 (1965) 993.

19) R. Nathans and S. J. Pickart: J. Phys. Chem. Solids 25 (1964) 183.

20) R. J. Weiss and A. S. Marotta: J. Phys. Chem. Solids 9 (1959) 302.

21) Y. Shirakawa: Sci. Rep. Tohoku Univ. 27 (1939) 485.

22) R. M. Bozorth: Ferromagnetism (D. Van Nostrand, Prinston 1951) p447.

Figure Captions

Fig. 1 The lattice constant versus x of $Fe_{65}(Ni_{1-x}Mn_x)35$ ternary alloys at room temperature. The left arrow indicates the composition which has the Curie temperature at room temperature. The right arrow indicates the composition which has the Neel temperature at room temperature.

Fig. 2 σ and $1/\chi$ versus temperature of FeNiMn alloys at 8600 Oe. Numbers of two figures indicate a composition, for example, 05 corresponding to x=0.05.

Fig. 3 σ versus H of FeNiMn alloys at 4.2°K.

Fig. 4 The effective Bohr magneton number of FeNiMn alloys obtained from the Curie-Weiss constant and the mean magneton number of FeNiMn alloys at 4.2°K as a function of x and mean electron concentration (N). The mean magneton number of FeNi alloys is also given as a function of N (according to Crangle and Hallam[13]).

Fig. 5 The Néel temperature and the Curie temperature of FeNiMn alloys as a function of mean electron concentration (N) and x. The Neel temperature of FeMn alloys and the Curie temperature of FeNi alloys are also given as a function of N.

Fig. 6 σ and $1/\chi$ versus temperature of FeNiMn alloys of x= 0.35, 0.40 and 0.50 at10000 Oe.

Fig. 7 χ versus temperature of FeNiMn alloys of x=0.50, 0.60, 0.70, 0.90 and 1.00 (FeMn) at 8600 Oe.

Fig. 8 σ and $1/\chi$ versus temperature of FeNiMn alloys of x=0.30 at10000 Oe.

Table I

Results of chemical analysis of $Fe_{65}(Ni_{1-x}Mn_x)_{35}$ alloys and mean concentration of outer shell electrons (N).

Sample Number	Ni	Mn	Fe	x	N
00	34.82%	0.03%	65.14%	0.0	8.695
05	33.27	1.59	65.20	0.046	8.654
09	31.50	3.06	65.43	0.089	8.600
12	30.48	4.35	65.15	0.124	8.565
16	29.15	5.56	65.28	0.160	8.527
19	27.80	6.53	65.65	0.190	8.489
23	26.73	7.84	65.41	0.226	8.455
30	23.93	10.03	65.86	0.295	8.364
35	22.21	12.10	65.67	0.352	8.322
40	20.60	13.96	65.41	0.404	8.270
50	16.95	17.07	65.97	0.502	8.167
60	13.66	20.74	65.60	0.603	8.066
70	10.12	23.93	65.95	0.703	7.963
90	3.43	30.61	65.95	0.899	7.761
FeMn	0.0				

Fig. 1

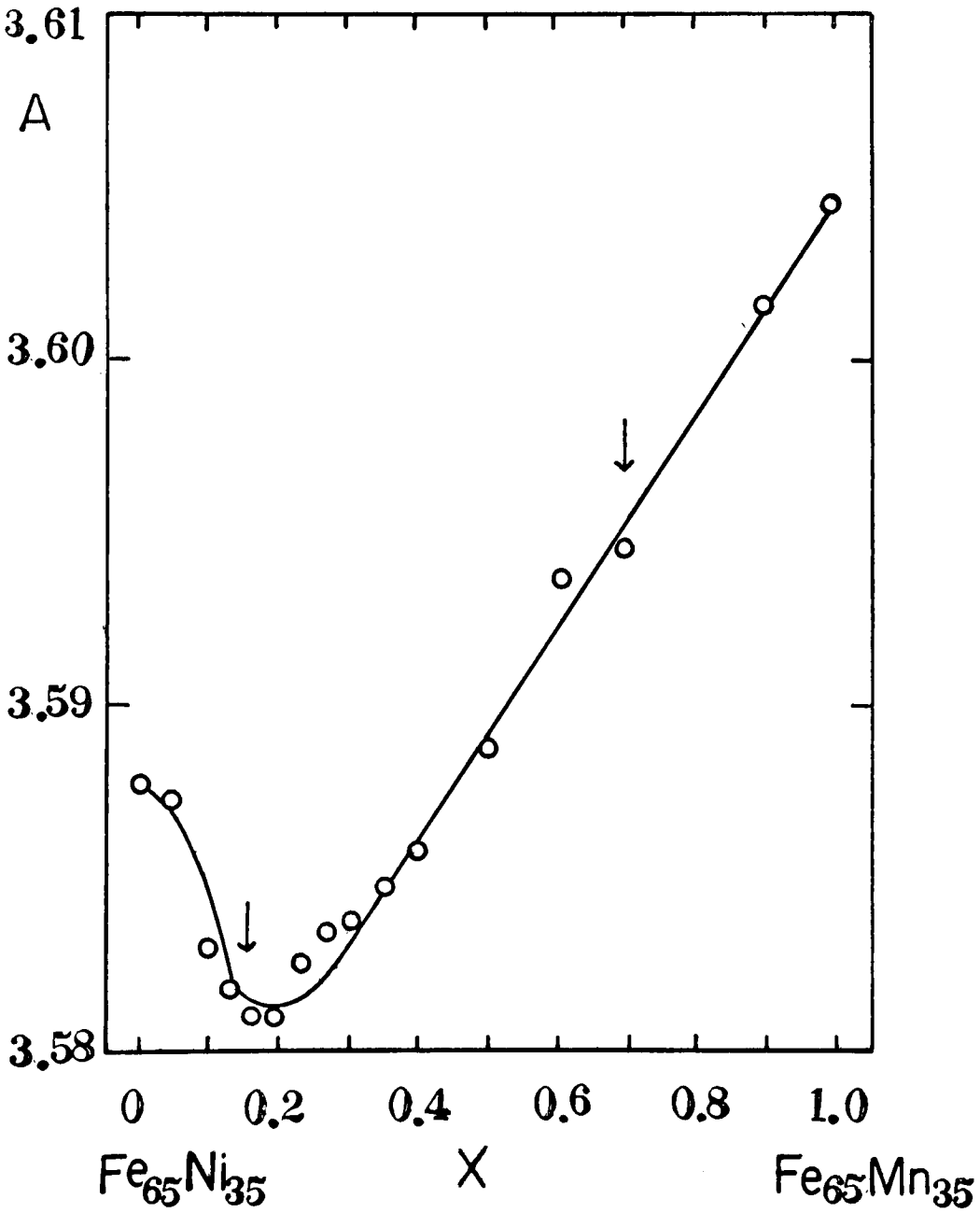

Fig. 2

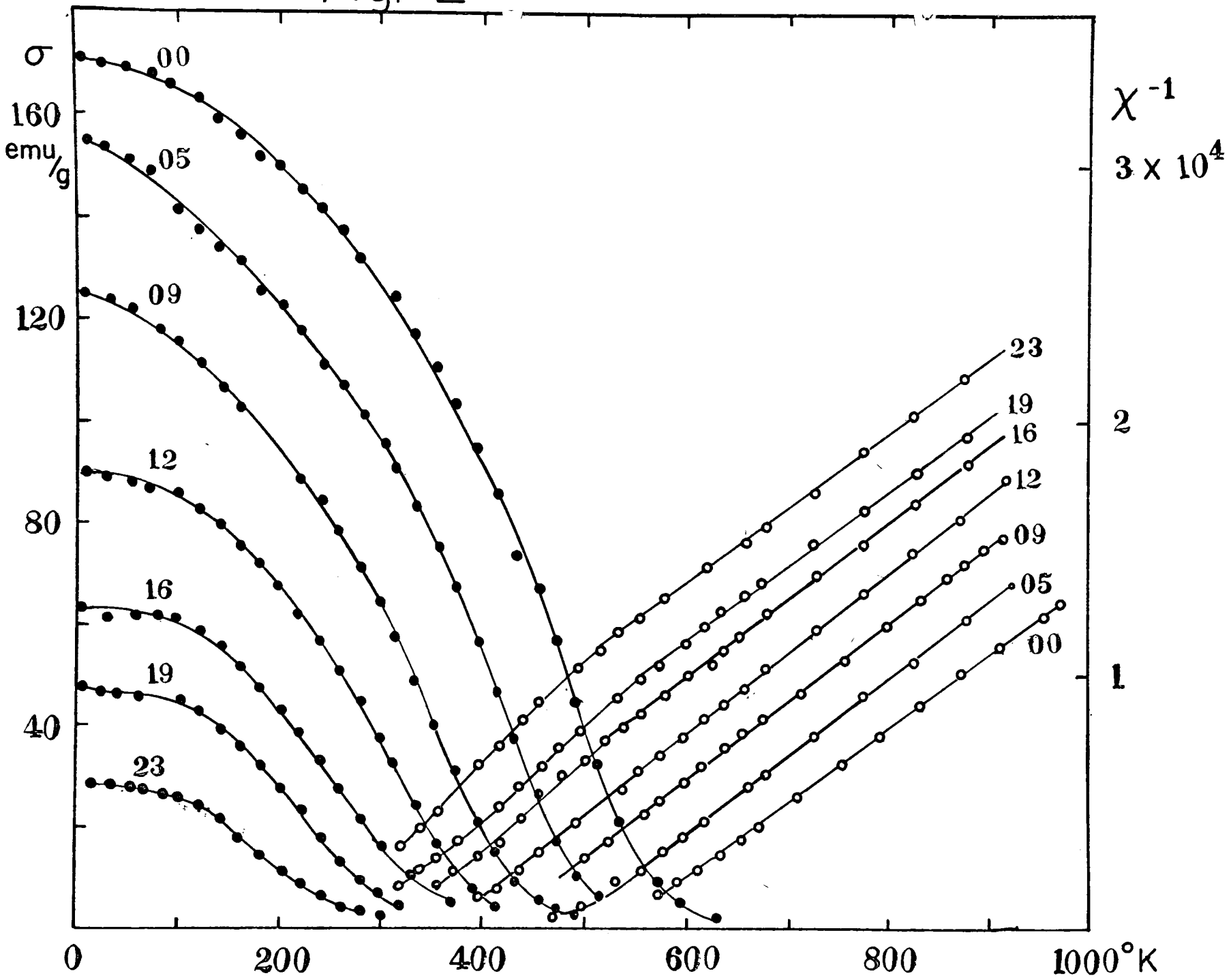
σ
160
emu/g
120
80
40
00
05
09
12
16
19
23
χ⁻¹
3 x 10⁴
2
1
0
200
400
600
800
1000°K

Fig. 3

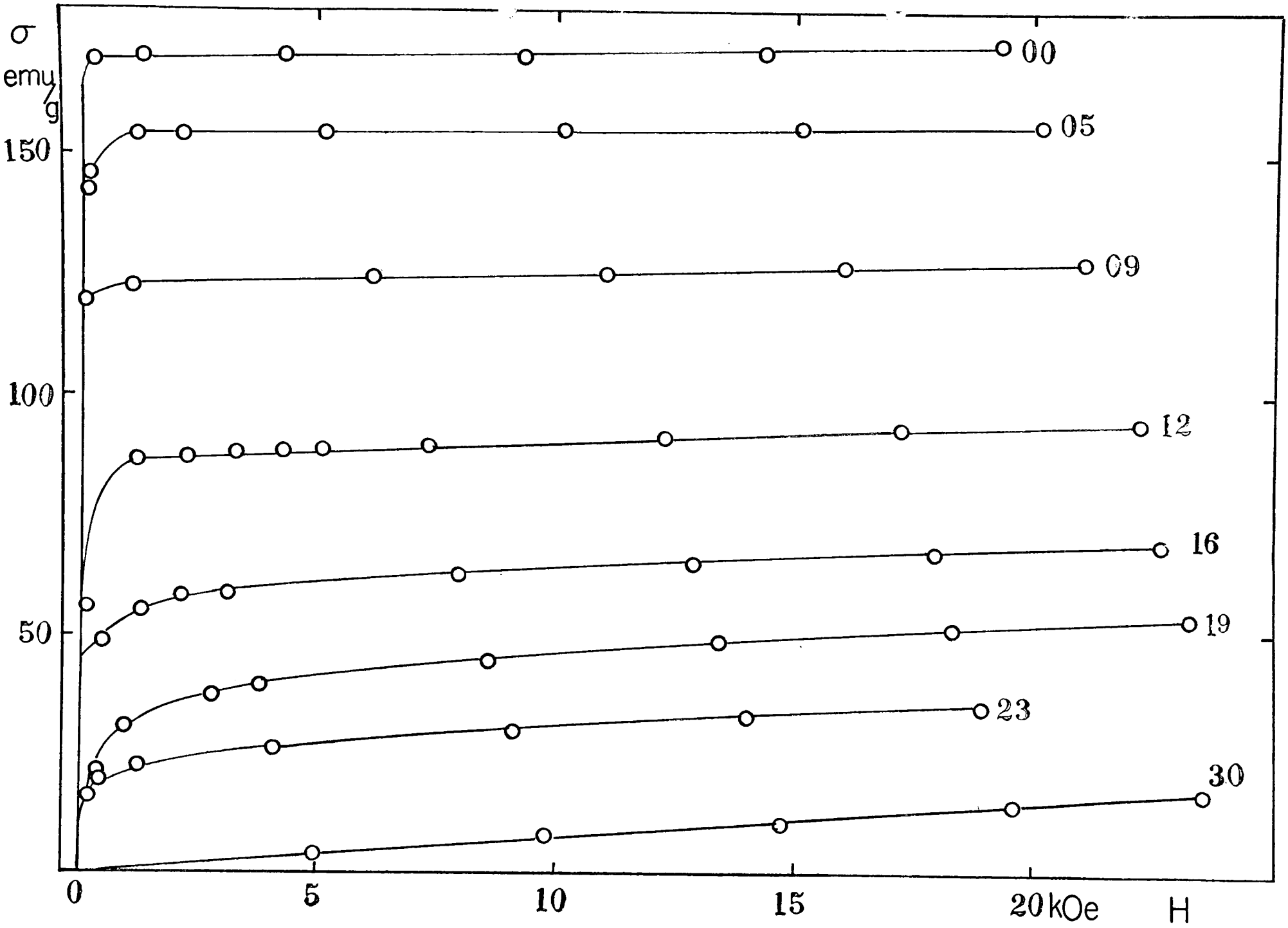

Fig. 4

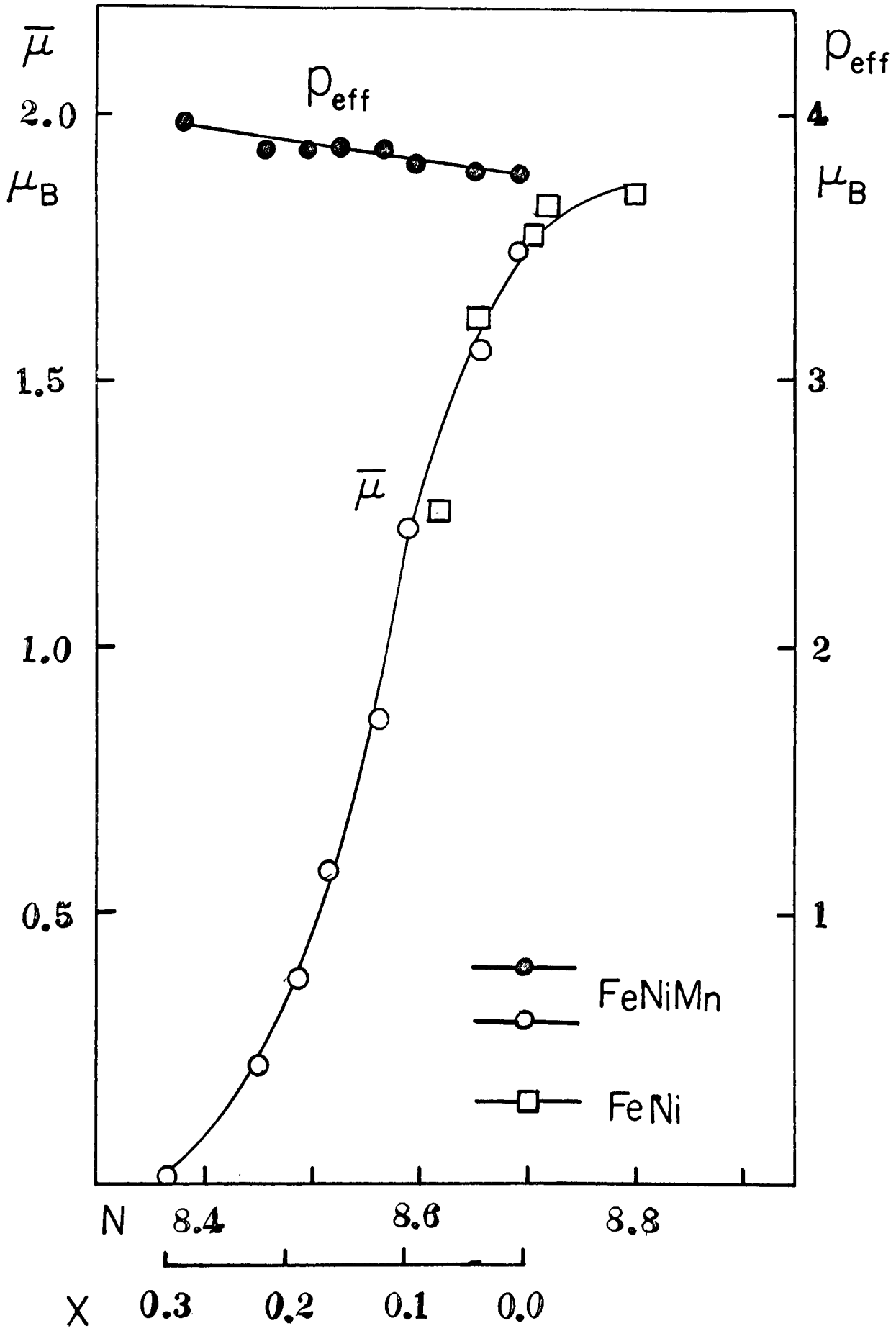
$\bar{\mu}$
p_{eff}
2.0
μ_B
1.5
1.0
0.5
p_{eff}
4
μ_B
3
2
1
$\bar{\mu}$
FeNiMn
FeNi
N
8.4
8.6
8.8
X
0.3
0.2
0.1
0.0

Fig. 5

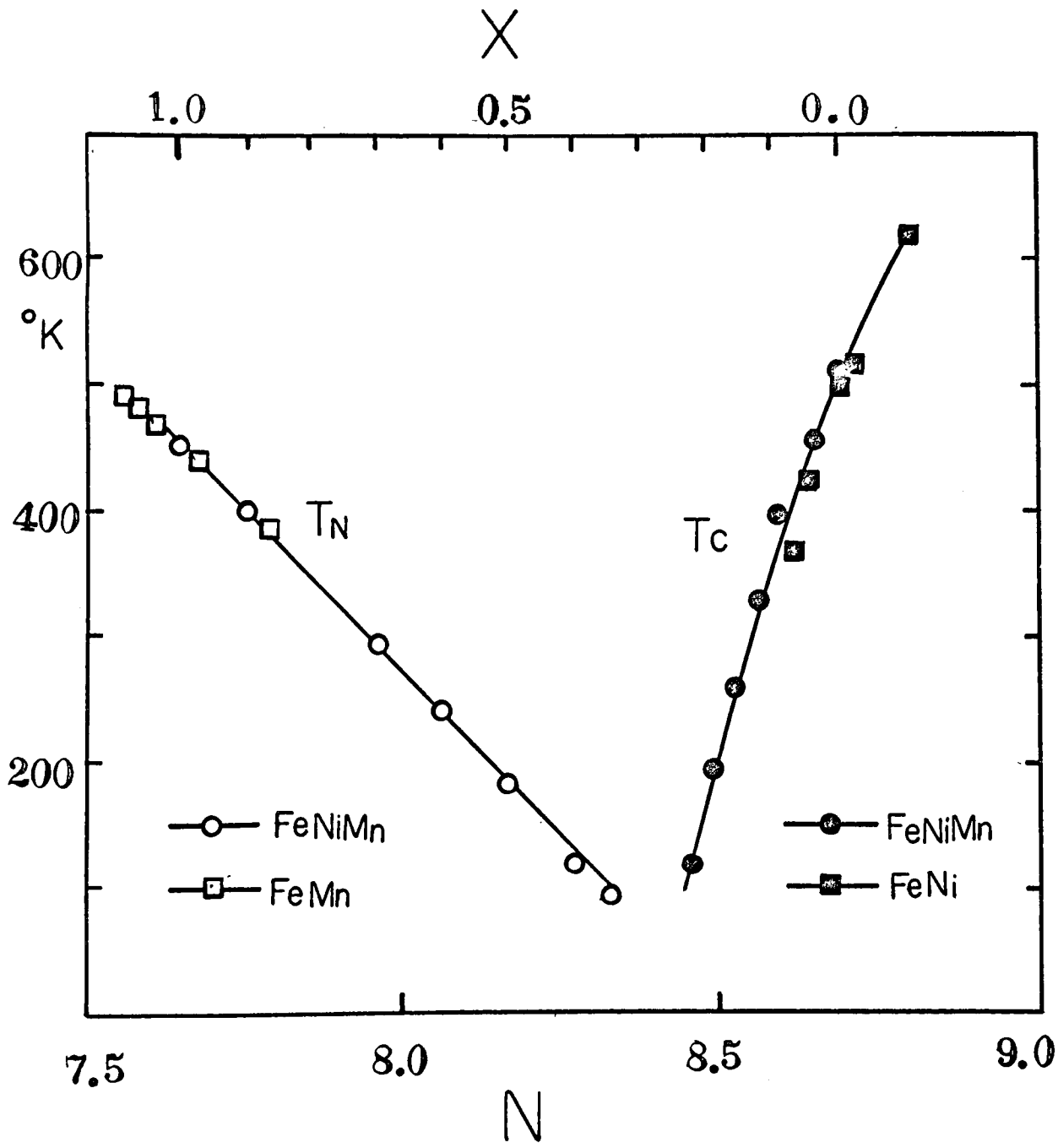
X
1.0
0.5
0.0
600
°K
400
200
T_N
Tc
FeNiMn
FeMn
FeNiMn
FeNi
7.5
8.0
8.5
9.0
N

Fig. 6

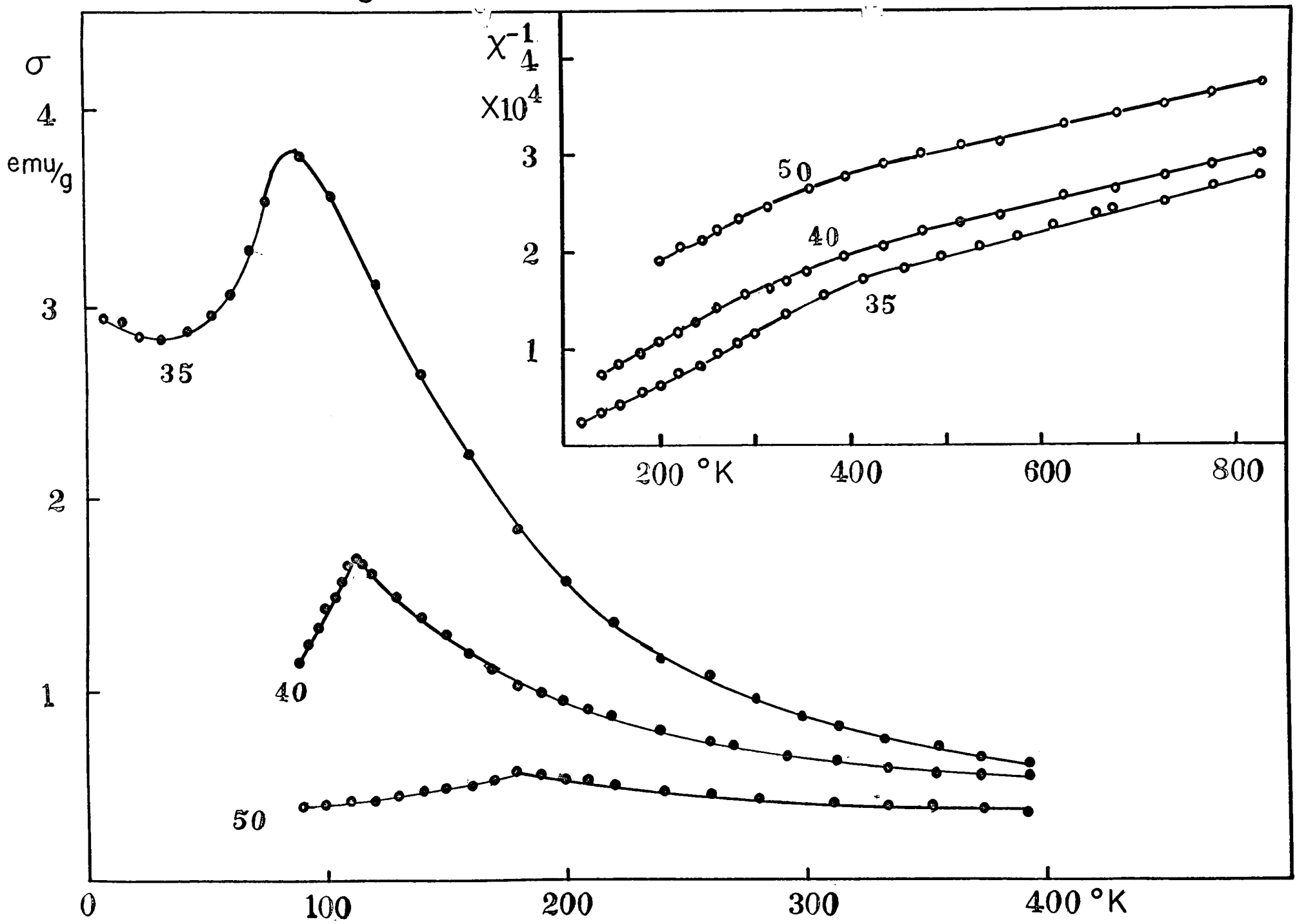
σ
4
emu/g
3
2
1
35
40
50
0
100
200
300
400 °K
χ^{-1}_4
$\times 10^4$
3
2
1
50
40
35
200 °K
400
600
800

Fig. 7

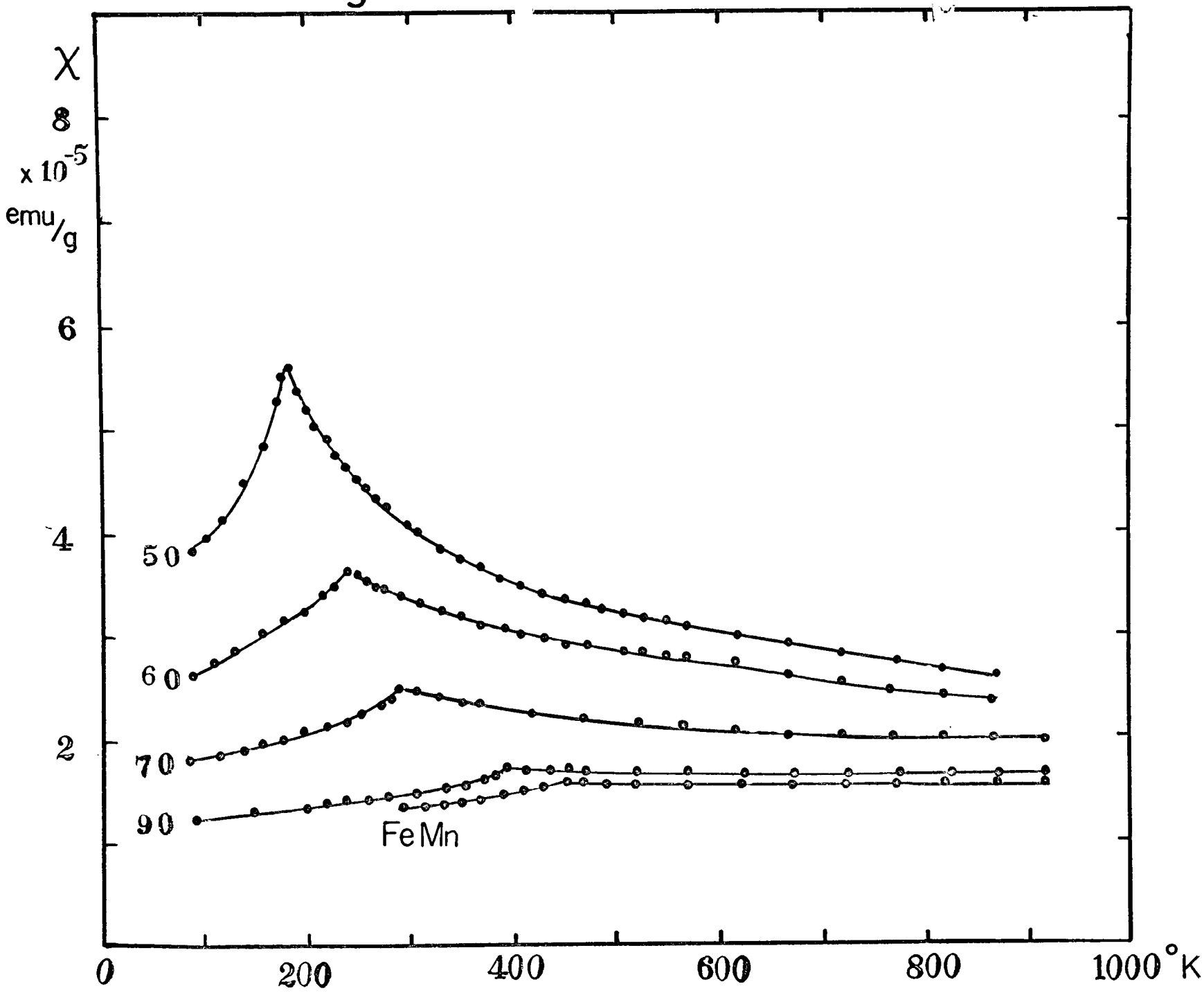

Fig. 8